Supplementary Information

How Oxidation State and Lattice Distortion influence the Oxygen Evolution Activity in Acid of Iridium Double Perovskites

María Retuerto[1,*], Laura Pascual[2], Oriol Piqué[3], Paula Kayser[4], Mohamed Abdel Salam[5], Mohamed Mokhtar[5], José Antonio Alonso[4], Miguel Peña[1], Federico Calle-Vallejo[3], Sergio Rojas[1,*]

[1]*Grupo de Energía y Química Sostenibles, Instituto de Catálisis y Petroleoquímica, CSIC. C/Marie Curie 2, 28049, Madrid, Spain*

[2]*Instituto de Catálisis y Petroleoquímica, CSIC. C/Marie Curie 2, 28049, Madrid, Spain*

[3]*Departament de Ciència de Materials i Química Física & Institut de Química Teòrica i Computacional (IQTCUB), Universitat de Barcelona, Martí i Franquès 1, 08028 Barcelona, Spain*

[4]*Instituto de Ciencia de Materiales de Madrid, CSIC. C/ Sor Juana Inés de la Cruz 3, 28049 Madrid, Spain*

[5]*Department of Chemistry, Faculty of Science, King Abdulaziz University, P.O Box 80200-Jeddah 21589, Saudi Arabia*

Table of Contents

S1. Additional computational details

The bulk of Sr_2MIrO_6 perovskites was modelled with a periodic cell containing 4 formula units of Sr_2MIrO_6, where all atoms were allowed to relax in all directions. A plane-wave cutoff of 400 eV was used along with an electronic temperature of 0.2 eV to facilitate convergence, extrapolating the total energies to 0 K. The search for minimum-energy structures was performed using the conjugate-gradient optimization scheme, with iterations carried out until the maximal force on any atom was below 0.05 eV $Å^{-1}$. Monkhorst-Pack[1] meshes of 4×4×4 were used to carry out the numerical integration in the reciprocal space. The Sr_2MIrO_6 perovskites were modelled in their (100) surface facet, since it is the thermodynamically most stable one and likely the most abundant. This practice is common when simulating oxide electrocatalysts for the OER.[2–4] Monkhorst-Pack meshes with 4×4×1 k-points were used for all modelled perovskites. The slab models contained eight layers (which contain 8 formula units in total), in which the topmost four and the adsorbates were allowed to relax in all directions, while the bottommost four were fixed at the bulk equilibrium distances to provide an adequate simulation of the subsurface region. The distance between repeated images in the vertical direction was larger than 13 Å. The converged geometries appear in section S10. Isolated molecules were calculated in boxes of 9×10×11 $Å^3$, using an electronic temperature of 0.001 eV with further extrapolation to 0 K and considering only the gamma point. All bulk and slab calculations were spin-unrestricted and considered all possible antiferromagnetic arranges (i.e. in different planes) of the spins. We do not expect important changes when simulating all perovskites in their antiferromagnetic phase (corresponding to the systems at 0 K) or all of them in their paramagnetic phase (corresponding to the systems above the Néel temperature), as the trends are based on adsorption energies in which the perovskite slabs appear as reactants and products. However, we note that this needs not be the case for other properties.[5] We did not perform spin-orbit coupling calculations, as those are not customary in electrocatalysis, not even for heavy elements such as Ir or Au (see again 2–4). Spin-orbit coupling is mandatory for the assessment of certain physical properties, but not for adsorption energies.

S2. Computational data, δ–ε optimization and Bader charges

In Table S1 we show the adsorption free energies of all the adsorbed intermediates of the OER (*O, *OH, *OOH) for all the studied Sr_2MIrO_6 perovskites. Moreover, the electrocatalytic symmetry index (ESSI) and the calculated OER overpotential are also provided. In the last column of Table S2 we show the average Bader atomic charges[6] present in Ir in the double perovskite slabs. Extracting oxidation numbers from atomic charges can be misleading and experts have advised not to do it,[7,8] so only the trends and not the actual values are to be analyzed. The trends hint toward more oxidized Ir centers in the order of M = Ni > Co > Fe > Sc, in consonance with the experimental observations (Figure 1a in the article).

Table S1. Free energies of adsorption of *O, *OH and *OOH (ΔG_O, ΔG_{OH}, ΔG_{OOH}, in eV), electrochemical-step symmetry index (ESSI, in V), calculated OER overpotentials (η_{OER}, in V), and average number of d electrons on Ir centers at the surface, for all the studied double perovskites.

Sr_2MIrO_6	ΔG_O	ΔG_{OH}	ΔG_{OOH}	ESSI	η_{OER}	d electrons @ Ir
M = Ni	2.12	0.77	3.25	0.28	0.44	6.80
M = Co	1.63	0.00	3.40	0.31	0.40	6.85
M = Sc	1.48	0.41	3.50	0.49	0.79	6.93
M = Fe	1.51	0.30	3.50	0.54	0.75	6.90

In Equations S1-S4 we show how the parameters are introduced into Equations 5-8 from the main text.

$$\Delta G_1 = \Delta G_{OH} + \delta \quad \text{(S1)}$$

$$\Delta G_2 = \Delta G_O - \Delta G_{OH} + \delta \quad \text{(S2)}$$

$$\Delta G_3 = \Delta G_{OOH} - \Delta G_O - \delta + \varepsilon \quad \text{(S3)}$$

$$\Delta G_4 = \Delta G_{O_2} - \Delta G_{OOH} - \delta - \varepsilon \quad \text{(S4)}$$

We emphasize that the sum of Equations S1 to S4 is $\Delta G_{O_2} = 4.92$ eV, as in Equations 5-8 in the main text, which corresponds to the standard equlibrium potential ($E^0 = 1.23$ V) multiplied by the number of transferred electrons per catalytic cicle ($1.23\ \text{V} \times 4\text{e}^- = 4.92$ eV).

S3. X-ray powder diffraction (XRD)

Figure S1 shows the XRD diffractograms for Sr_2MIrO_6 (M = Ni, Co, Sc and Fe). All the samples are pure and exhibit the perovskite crystal structure. The inset of Figure S1 depicts the evolution of the volume of the unit cell, which increases with M in the order Co^{3+}< Fe^{3+}< Ni^{2+}< Sc^{3+}. This result shows that the size of the cell is determined by the ionic radii of the M cations and not by that of Ir^{6+}/Ir^{5+}, which would have given a different trend.[9]

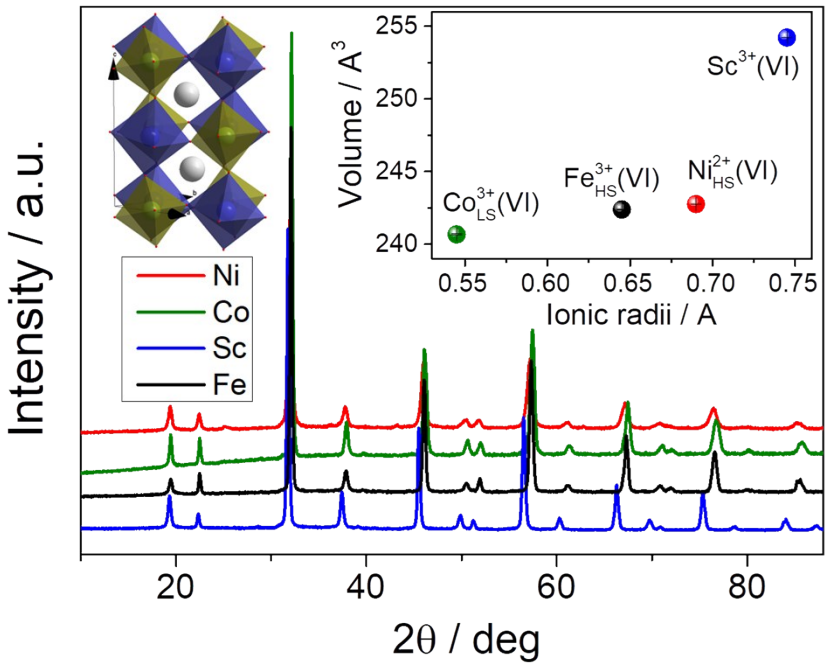

Figure S1. X-ray powder diffraction patterns for Sr_2MIrO_6 (M = Ni, Co, Sc and Fe) collected at room temperature with Cu-Kα radiation. Inset: Evolution of the cell volumes obtained from the Rietveld fits. LS refers to Low Spin configuration and HS to High Spin Configuration.

S4. Powder Neutron Diffraction (PND)

Table S2. Crystallographic parameters obtained from PND.*

	Space Group	**Monoclinic β angle**	**Oxygen Vacancies**	**Ir^{n+} (XAS & PND)**	**M^{n+} (XAS & PND)**	**<Ir-O>**	**<M-O>**
Sr_2NiIrO_6	$P2_1/n$	89.979(1)	0	6+	2 +	1.972(13)	1.986(12)
Sr_2CoIrO_6	$I2/m$	89.970(2)	0	6+/5+ (BVS +5.7)	3+/2+	1.95(1)	1.99(1)
Sr_2ScIrO_6	$P2_1/n$	89.9855(9)	0	5+	3+	1.99(1)	2.02(1)
Sr_2FeIrO_6	$I2/m$	89.986(2)	0	5+	3+	1.96(2)	1.98(2)

* from references [10,11]

S5. X-ray Photoemission Spectroscopy (XPS)

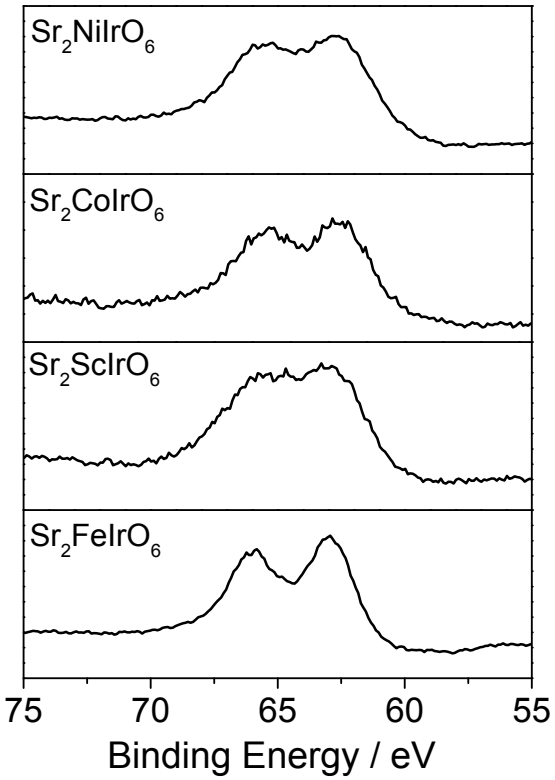

Figure S2. Ir 4f core-level region of the initial catalysts.

S6. Electrochemical measurements.

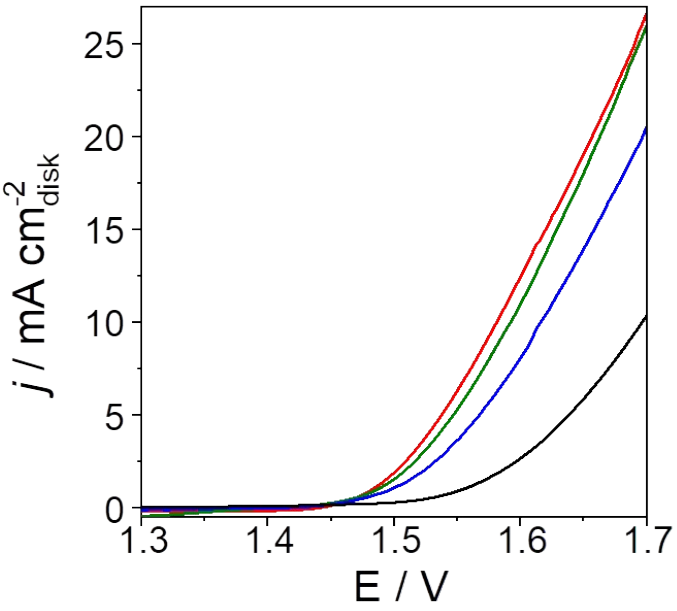

Figure S3. Current density *vs.* uncorrected potential for Sr_2MIrO_6 (M = Co, Ni, Sc, Fe).

Electrochemical impedance spectroscopy (EIS)

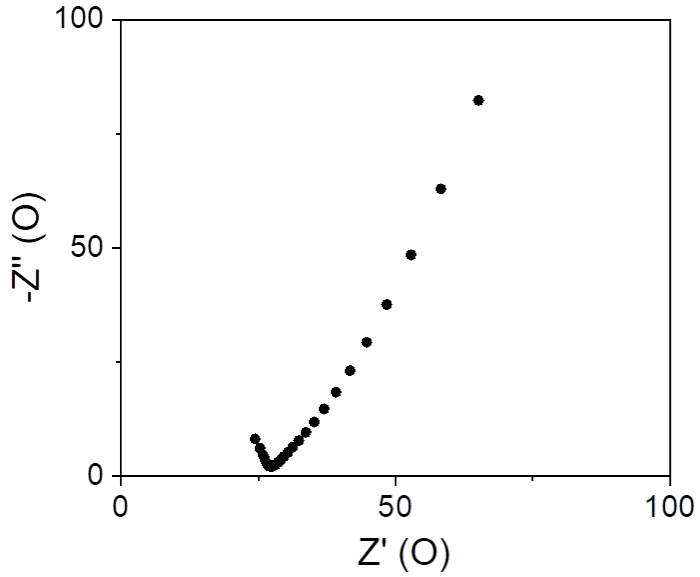

Figure S4. Nyquist plot from an electrochemical impedance spectroscopy experiment at open circuit voltage.

S7. OER trend as a function of the structural distortion.

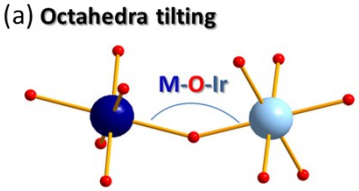

$$Oh_{tilting} = \frac{180 - < \text{M-O-Ir} >}{2}$$

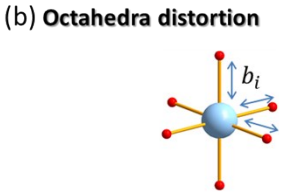

$$\Delta = \frac{1}{6}\sum\{(b_i - b_{av})/b_{av}\}^2$$

Figure S5. (a) Schematics of the tilting of the octahedra, with the M-O-Ir angles detailed. (b) Schematic view of the IrO_6 octahedral distortions. b_i: individual Ir-O distances. b_{av}: average <Ir-O> distances.

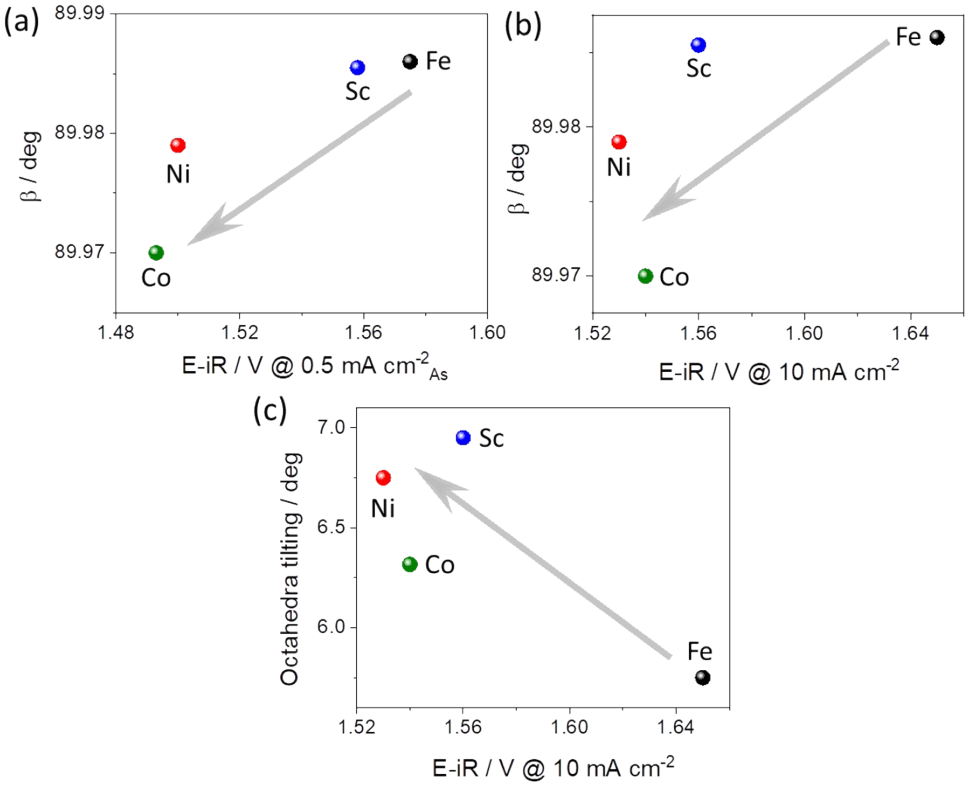

Figure S6. (a) Activity trend on Sr_2MIrO_6 (M = Co, Ni, Sc, Fe) with the monoclinic ß angle. (b) Evolution of the current density with the monoclinic ß angle. (c) Evolution of the current density with the tilting of the octahedra, calculated as 180°-<M-O-Ir>°/2. The arrows point toward higher OER catalytic activities.

S8. Transmission Electron Microscopy (TEM)

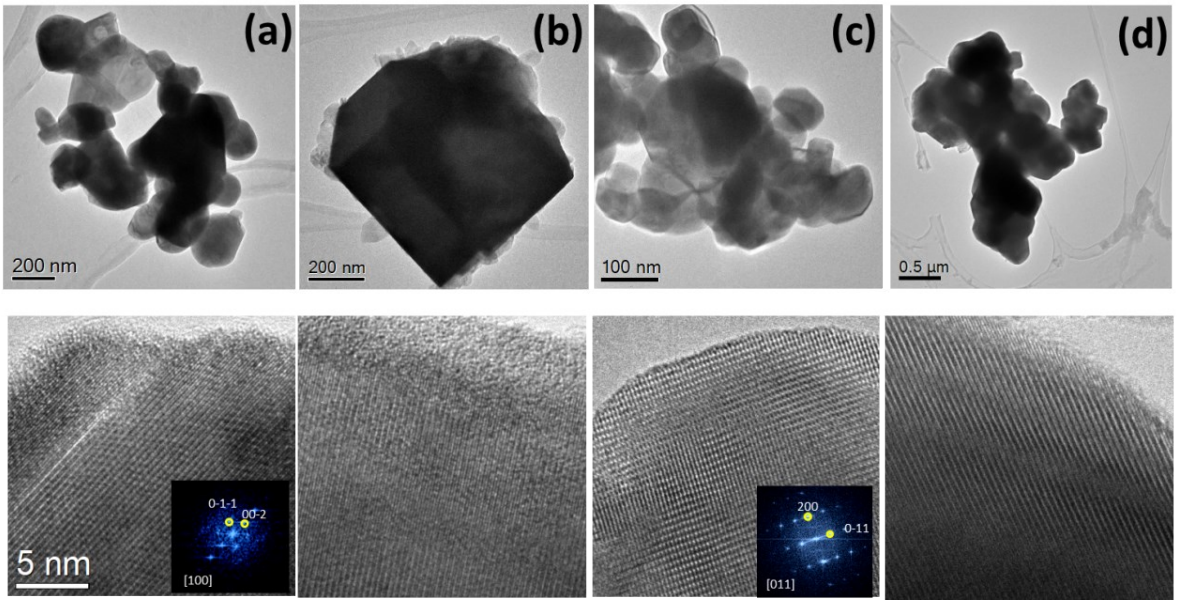

Figure S7. TEM and HRTEM images of the initial Sr_2MIrO_6 (a) M = Ni, (b) Co, (c) Sc and (d) Fe.

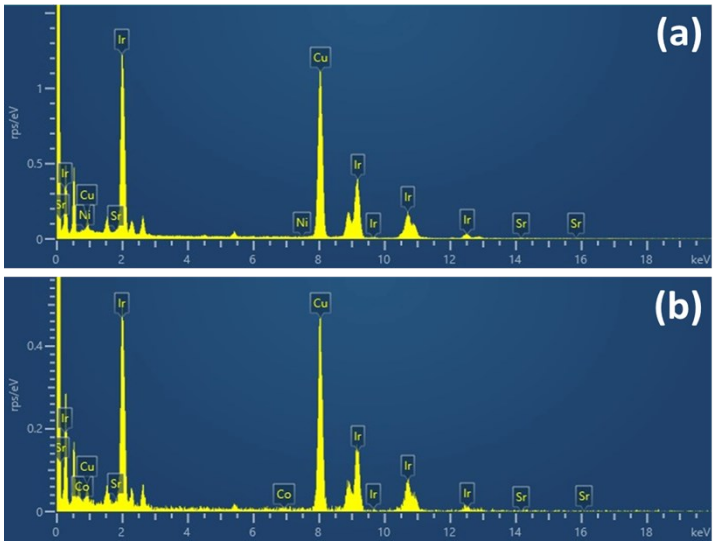

Figure S8. EDX analysis of (a) Sr_2NiIrO_6 and (b) Sr_2CoIrO_6 after 50 cycles of OER reaction.

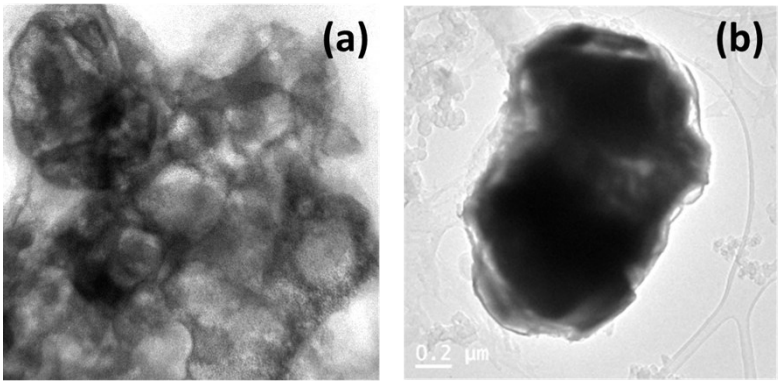

Figure S9. TEM images of (a) Sr_2NiIrO_6 and (b) Sr_2CoIrO_6 after 50 OER cycles in acid media.

S9. Surface Area Calculation

The mass specific surface areas, A_S, were determined using a spherical geometry approximation. By TEM we measured the diameter (d) of the particles (Figure S2), and calculated the volume/area diameter ($d_{v/a}$) as $d_{v/a}= \Sigma d^3/\Sigma d^2$. A_S was determined using the following formula:

$$A_s = \sum \pi d^2 \Big/ \sum \tfrac{1}{6} \rho \pi d^3 = 6 \sum d^2 \Big/ \rho \sum d^3 = 6/\rho d_{v/a} \quad \text{(S5)}$$

where ρ is the oxide bulk density following the formula:

$$\rho = \frac{Mw \times Z}{N_A \times V_{f.u}} \quad \text{(S6)}$$

where Mw is the molecular weight, Z is the number of formula units per cell (Z = 2 for P$2_1/n$ and Z = 2 for I$2/m$), N_A is Avogadro's number, and $V_{f.u.}$ is the volume of the formula unit.

N_2 adsorption-desorption isotherms were recorded at liquid N_2 temperature with a Micromeritics ASAP 2000 apparatus to evaluate textural properties. The samples were degassed at 140 °C under vacuum for 24 h. The specific areas were calculated by applying the BET method within the relative pressure range P/P_0 = 0.05-0.30.

The electrochemically active surface area (ECSA) was calculated by the double-layer capacitance of the perovskites without adding active carbon. We performed cyclic voltammograms at different velocities close to the "*open circuit potential*" in an inert gas, where the measured currents are due to double-layer charging. ECSA was recorded at 200, 100, 50, 20 and 10 mV s^{-1} between 0.7 and 0.9 V *vs.* RHE. The double-layer charging current (i_c) is equal to the product of the scan rate (ν) and the double-layer capacitance (C_{dl}): $i_c= \nu C_{dl}$. If i_c is plotted as a function of ν, then the slope is C_{dl}, and ECSA will be ECSA = C_{dl}/ C_S; where C_S is the specific capacitance of an atomically flat planar surface of the material per unit area under identical electrolyte conditions. Since this value is not well established for oxides, we used 0.06 mF/cm^2 as done in previous works for 0.1 M $HClO_4$.[12,13] Table S2 shows the results obtained for ECSA and BET for several perovskites compared to the values obtained for A_S.

Table S3. Surface area calculated from BET, ECSA and TEM (A_S).

	BET /m^2g^{-1}	**ECSA / m^2g^{-1}**	**A_S /m^2g^{-1}**
Sr_2NiIrO_6	-	6(2)	2.9
Sr_2CoIrO_6	1.2	-	1.3
Sr_2ScIrO_6	-	-	6.8
Sr_2FeIrO_6	0.3	7.4(2)	1.6

S10. Inductively Coupled Plasma Optical Emission Spectrometry (ICP-OES)

An ICP-OES Analytik Jena PQ 9000 spectrometer was used for the analyses. For the experiments we used a 1 mm thin graphite wafer (geometric surface of 100 mm^2) as working electrode and we deposited 2 mg of electrocatalyst on both faces.

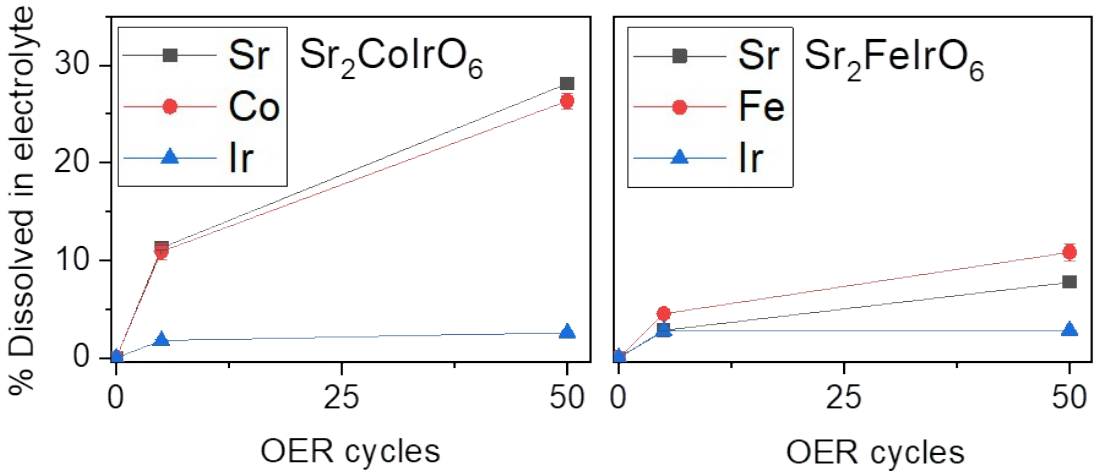

Figure S10. ICP-OES analysis of the electrolyte of Sr_2CoIrO_6 and Sr_2FeIrO_6 after 0, 5 and 50 OER reaction cycles, showing the degree of dissolution of Sr, M (Co and Fe) and Ir for both samples.

S11. Optimized geometries.

M = Co

1.00000000000000

8.0299997330000004 0.0000000000000000 0.0000000000000000

0.0000000000000000 8.0299997330000004 0.0000000000000000

0.0000000000000000 0.0000000000000000 28.0599994658999989

Sr Co Ir O

16 8 8 48

Selective dynamics

Direct

0.0000000000000000 0.0000000000000000 0.0000000000000000 F F F

-0.0000000000000000 0.0000000000000000 0.2863735289011256 T T T

0.0000000000000000 0.0000000000000000 0.1430862400000024 F F F

-0.0000000000000000 0.0000000000000000 0.4324090481994619 T T T

0.0000000000000000 0.5000000000000000 0.0000000000000000 F F F

-0.0000000000000000 0.5000000000000000 0.2863735289011256 T T T

0.0000000000000000 0.5000000000000000 0.1430862400000024 F F F

-0.0000000000000000 0.5000000000000000 0.4324090481994619 T T T

0.5000000000000000 0.0000000000000000 0.0000000000000000 F F F

0.5000000000000000 0.0000000000000000 0.2863735289011256 T T T

0.5000000000000000 0.0000000000000000 0.1430862400000024 F F F

0.5000000000000000 0.0000000000000000 0.4324090481994619 T T T

0.5000000000000000 0.5000000000000000 0.0000000000000000 F F F

0.5000000000000000 0.5000000000000000 0.2863735289011256 T T T

0.5000000000000000 0.5000000000000000 0.1430862400000024 F F F

0.5000000000000000 0.5000000000000000 0.4324090481994619 T T T

0.2500000000000000 0.2500000000000000 0.2146293670000006 F F F

0.2500000000000000 0.2500000000000000 0.4989217147364486 T T T

0.2500000000000000 0.7500000000000000 0.0715431200000012 F F F

0.2500000000000000 0.7500000000000000 0.3543705047034249 T T T

0.7500000000000000 0.2500000000000000 0.0715431200000012 F F F

0.7500000000000000 0.2500000000000000 0.3543705047034249 T T T

0.7500000000000000 0.7500000000000000 0.2146293670000006 F F F

0.7500000000000000 0.7500000000000000 0.4989217147364486 T T T

0.2500000000000000 0.2500000000000000 0.0715431200000012 F F F

0.2500000000000000 0.2500000000000000 0.3573548472806761 T T T

0.2500000000000000 0.7500000000000000 0.2146293670000006 F F F

0.2500000000000000 0.7500000000000000 0.4993247389665925 T T T

0.7500000000000000 0.2500000000000000 0.2146293670000006 F F F

0.7500000000000000 0.2500000000000000 0.4993247389665925 T T T

0.7500000000000000 0.7500000000000000 0.0715431200000012 F F F

0.7500000000000000 0.7500000000000000 0.3573548472806761 T T T

0.2500000000000000 0.2500000000000000 0.0008654109999995 F F F

0.2500000000000000 0.2500000000000000 0.2868778367334923 T T T

0.0035860249999971 0.2500000000000000 0.0715431200000012 F F F

0.0025156587968238 0.2500000000000000 0.3574888148086809 T T T

0.2500000000000000 0.0035860249999971 0.0715431200000012 F F F

0.2500000000000000 0.0025156587968238 0.3574888148086809 T T T

0.2500000000000000 0.2500000000000000 0.1422208250000025 F F F

0.2500000000000000 0.2500000000000000 0.4276455485928497 T T T

0.9964139459999970 0.2500000000000000 0.2146293670000006 F F F

0.9942574827040969 0.2500000000000000 0.5007422046083854 T T T

0.2500000000000000 0.9964139459999970 0.2146293670000006 F F F

0.2500000000000000 0.9942574827040969 0.5007422046083854 T T T

0.2500000000000000 0.7500000000000000 0.2849370409547679 T T T

0.2500000000000000 0.7500000000000000 0.0008654109999995 F F F

0.9964139459999970 0.7500000000000000 0.0715431200000012 F F F

0.9974843122031702 0.7500000000000000 0.3574888148086809 T T T

0.2500000000000000 0.4964139759999995 0.0715431200000012 F F F

0.2500000000000000 0.4974843422031728 0.3574888148086809 T T T

0.2500000000000000 0.7500000000000000 0.1439516539999985 F F F

0.2500000000000000 0.7500000000000000 0.4300448820059606 T T T

0.0035860249999971 0.7500000000000000 0.2146293670000006 F F F

0.0057424882958971 0.7500000000000000 0.5007422046083854 T T T

0.2500000000000000 0.5035860540000030 0.2146293670000006 F F F

0.2500000000000000 0.5057425172959031 0.5007422046083854 T T T
0.7500000000000000 0.2500000000000000 0.2849370409547679 T T T
0.7500000000000000 0.2500000000000000 0.0008654109999995 F F F
0.4964139759999995 0.2500000000000000 0.0715431200000012 F F F
0.4974843422031728 0.2500000000000000 0.3574888148086809 T T T
0.7500000000000000 0.9964139459999970 0.0715431200000012 F F F
0.7500000000000000 0.9974843122031702 0.3574888148086809 T T T
0.7500000000000000 0.2500000000000000 0.1439516539999985 F F F
0.7500000000000000 0.2500000000000000 0.4300448820059606 T T T
0.5035860540000030 0.2500000000000000 0.2146293670000006 F F F
0.5057425172959031 0.2500000000000000 0.5007422046083854 T T T
0.7500000000000000 0.0035860249999971 0.2146293670000006 F F F
0.7500000000000000 0.0057424882958971 0.5007422046083854 T T T
0.7500000000000000 0.7500000000000000 0.0008654109999995 F F F
0.7500000000000000 0.7500000000000000 0.2868778367334923 T T T
0.5035860540000030 0.7500000000000000 0.0715431200000012 F F F
0.5025156877968298 0.7500000000000000 0.3574888148086809 T T T
0.7500000000000000 0.5035860540000030 0.0715431200000012 F F F
0.7500000000000000 0.5025156877968298 0.3574888148086809 T T T
0.7500000000000000 0.7500000000000000 0.1422208250000025 F F F
0.7500000000000000 0.7500000000000000 0.4276455485928497 T T T
0.4964139759999995 0.7500000000000000 0.2146293670000006 F F F
0.4942575127040993 0.7500000000000000 0.5007422046083854 T T T
0.7500000000000000 0.4964139759999995 0.2146293670000006 F F F
0.7500000000000000 0.4942575127040993 0.5007422046083854 T T T

M = Ni

1.00000000000000

8.0399999999999991 0.0000000000000000 0.0000000000000000

0.0000000000000000 8.0399999999999991 0.0000000000000000

0.0000000000000000 0.0000000000000000 28.0949434254000003

Sr Ni Ir O

16 8 8 48

Selective dynamics

Direct

0.0000000000000000 0.0000000000000000 0.0000000000000000 F F F
0.0000000000000000 0.0000000000000000 0.2868912798347441 T T T
0.0000000000000000 0.0000000000000000 0.1430862400000024 F F F
0.0000000000000000 0.0000000000000000 0.4329179999086473 T T T
0.0000000000000000 0.5000000000000000 0.0000000000000000 F F F
0.0000000000000000 0.5000000000000000 0.2868912798347441 T T T
0.0000000000000000 0.5000000000000000 0.1430862400000024 F F F
0.0000000000000000 0.5000000000000000 0.4329179999086473 T T T
0.5000000000000000 0.0000000000000000 0.0000000000000000 F F F
0.5000000000000000 0.0000000000000000 0.2868912798347441 T T T
0.5000000000000000 0.0000000000000000 0.1430862400000024 F F F
0.5000000000000000 0.0000000000000000 0.4329179999086473 T T T
0.5000000000000000 0.5000000000000000 0.0000000000000000 F F F
0.5000000000000000 0.5000000000000000 0.2868912798347441 T T T
0.5000000000000000 0.5000000000000000 0.1430862400000024 F F F
0.5000000000000000 0.5000000000000000 0.4329179999086473 T T T
0.2500000000000000 0.2500000000000000 0.2146293670000006 F F F
0.2500000000000000 0.2500000000000000 0.5019763070505872 T T T
0.2500000000000000 0.7500000000000000 0.0715431200000012 F F F
0.2500000000000000 0.7500000000000000 0.3586092555489874 T T T
0.7500000000000000 0.2500000000000000 0.0715431200000012 F F F
0.7500000000000000 0.2500000000000000 0.3586092555489874 T T T
0.7500000000000000 0.7500000000000000 0.2146293670000006 F F F
0.7500000000000000 0.7500000000000000 0.5019763070505872 T T T
0.2500000000000000 0.2500000000000000 0.0715431200000012 F F F
0.2500000000000000 0.2500000000000000 0.3576560285075872 T T T
0.2500000000000000 0.7500000000000000 0.2146293670000006 F F F
0.2500000000000000 0.7500000000000000 0.5016348415372999 T T T
0.7500000000000000 0.2500000000000000 0.2146293670000006 F F F
0.7500000000000000 0.2500000000000000 0.5016348415372999 T T T
0.7500000000000000 0.7500000000000000 0.0715431200000012 F F F
0.7500000000000000 0.7500000000000000 0.3576560285075872 T T T

0.2500000000000000 0.2500000000000000 0.0008654109999995 F F F
0.2500000000000000 0.2500000000000000 0.2876442558733089 T T T
0.0035860249999971 0.2500000000000000 0.0715431200000012 F F F
0.0054082279939845 0.2500000000000000 0.3570355378127868 T T T
0.2500000000000000 0.0035860249999971 0.0715431200000012 F F F
0.2500000000000000 0.0054082279939845 0.3570355378127868 T T T
0.2500000000000000 0.2500000000000000 0.1422208250000025 F F F
0.2500000000000000 0.2500000000000000 0.4279680330594950 T T T
0.9964139459999970 0.2500000000000000 0.2146293670000006 F F F
0.9893137316158638 0.2500000000000000 0.5018439047651715 T T T
0.2500000000000000 0.9964139459999970 0.2146293670000006 F F F
0.2500000000000000 0.9893137316158638 0.5018439047651715 T T T
0.2500000000000000 0.7500000000000000 0.2837931031161391 T T T
0.2500000000000000 0.7500000000000000 0.0008654109999995 F F F
0.9964139459999970 0.7500000000000000 0.0715431200000012 F F F
0.9945917430060097 0.7500000000000000 0.3570355378127868 T T T
0.2500000000000000 0.4964139759999995 0.0715431200000012 F F F
0.2500000000000000 0.4945917730060120 0.3570355378127868 T T T
0.2500000000000000 0.7500000000000000 0.1439516539999985 F F F
0.2500000000000000 0.7500000000000000 0.4272285358163882 T T T
0.0035860249999971 0.7500000000000000 0.2146293670000006 F F F
0.0106862393841305 0.7500000000000000 0.5018439047651715 T T T
0.2500000000000000 0.5035860540000030 0.2146293670000006 F F F
0.2500000000000000 0.5106862683841362 0.5018439047651715 T T T
0.7500000000000000 0.2500000000000000 0.2837931031161391 T T T
0.7500000000000000 0.2500000000000000 0.0008654109999995 F F F
0.4964139759999995 0.2500000000000000 0.0715431200000012 F F F
0.4945917730060120 0.2500000000000000 0.3570355378127868 T T T
0.7500000000000000 0.9964139459999970 0.0715431200000012 F F F
0.7500000000000000 0.9945917430060097 0.3570355378127868 T T T
0.7500000000000000 0.2500000000000000 0.1439516539999985 F F F
0.7500000000000000 0.2500000000000000 0.4272285358163882 T T T
0.5035860540000030 0.2500000000000000 0.2146293670000006 F F F
0.5106862683841362 0.2500000000000000 0.5018439047651715 T T T
0.7500000000000000 0.0035860249999971 0.2146293670000006 F F F
0.7500000000000000 0.0106862393841305 0.5018439047651715 T T T
0.7500000000000000 0.7500000000000000 0.0008654109999995 F F F
0.7500000000000000 0.7500000000000000 0.2876442558733089 T T T
0.5035860540000030 0.7500000000000000 0.0715431200000012 F F F
0.5054082569939903 0.7500000000000000 0.3570355378127868 T T T
0.7500000000000000 0.5035860540000030 0.0715431200000012 F F F
0.7500000000000000 0.5054082569939903 0.3570355378127868 T T T
0.7500000000000000 0.7500000000000000 0.1422208250000025 F F F
0.7500000000000000 0.7500000000000000 0.4279680330594950 T T T
0.4964139759999995 0.7500000000000000 0.2146293670000006 F F F
0.4893137616158661 0.7500000000000000 0.5018439047651715 T T T
0.7500000000000000 0.4964139759999995 0.2146293670000006 F F F
0.7500000000000000 0.4893137616158661 0.5018439047651715 T T T

M = Sc

1.00000000000000

8.1600000000000001 0.0000000000000000 0.0000000000000000

0.0000000000000000 8.1600000000000001 0.0000000000000000

0.0000000000000000 0.0000000000000000 28.5142709391999993

Sr Sc Ir O

16 8 8 48

Selective dynamics

Direct

0.0000000000000000 0.0000000000000000 0.0000000000000000 F F F
0.0000000000000000 -0.0000000000000000 0.2860915785622686 T T T
0.0000000000000000 0.0000000000000000 0.1430862400000024 F F F
0.0000000000000000 -0.0000000000000000 0.4328389065530059 T T T
0.0000000000000000 0.5000000000000000 0.0000000000000000 F F F
0.0000000000000000 0.5000000000000000 0.2860915785622686 T T T
0.0000000000000000 0.5000000000000000 0.1430862400000024 F F F
0.0000000000000000 0.5000000000000000 0.4328389065530059 T T T
0.5000000000000000 0.0000000000000000 0.0000000000000000 F F F

0.5000000000000000	-0.0000000000000000	0.2860915785622686	T	T	T
0.5000000000000000	0.0000000000000000	0.1430862400000024	F	F	F
0.5000000000000000	-0.0000000000000000	0.4328389065530059	T	T	T
0.5000000000000000	0.5000000000000000	0.0000000000000000	F	F	F
0.5000000000000000	0.5000000000000000	0.2860915785622686	T	T	T
0.5000000000000000	0.5000000000000000	0.1430862400000024	F	F	F
0.5000000000000000	0.5000000000000000	0.4328389065530059	T	T	T
0.2500000000000000	0.2500000000000000	0.2146293670000006	F	F	F
0.2500000000000000	0.2500000000000000	0.4984783984200058	T	T	T
0.2500000000000000	0.7500000000000000	0.0715431200000012	F	F	F
0.2500000000000000	0.7500000000000000	0.3561401276663140	T	T	T
0.7500000000000000	0.2500000000000000	0.0715431200000012	F	F	F
0.7500000000000000	0.2500000000000000	0.3561401276663140	T	T	T
0.7500000000000000	0.7500000000000000	0.2146293670000006	F	F	F
0.7500000000000000	0.7500000000000000	0.4984783984200058	T	T	T
0.2500000000000000	0.2500000000000000	0.0715431200000012	F	F	F
0.2500000000000000	0.2500000000000000	0.3580176028235175	T	T	T
0.2500000000000000	0.7500000000000000	0.2146293670000006	F	F	F
0.2500000000000000	0.7500000000000000	0.4974341873748597	T	T	T
0.7500000000000000	0.2500000000000000	0.2146293670000006	F	F	F
0.7500000000000000	0.2500000000000000	0.4974341873748597	T	T	T
0.7500000000000000	0.7500000000000000	0.0715431200000012	F	F	F
0.7500000000000000	0.7500000000000000	0.3580176028235175	T	T	T
0.2500000000000000	0.2500000000000000	0.0008654109999995	F	F	F
0.2500000000000000	0.2500000000000000	0.2888210346683538	T	T	T
0.0035860249999971	0.2500000000000000	0.0715431200000012	F	F	F
0.0065770248718115	0.2500000000000000	0.3578489359329504	T	T	T
0.2500000000000000	0.0035860249999971	0.0715431200000012	F	F	F
0.2500000000000000	0.0065770248718114	0.3578489359329504	T	T	T
0.2500000000000000	0.2500000000000000	0.1422208250000025	F	F	F
0.2500000000000000	0.2500000000000000	0.4280226560388691	T	T	T
0.9964139459999970	0.2500000000000000	0.2146293670000006	F	F	F
0.9916158561626814	0.2500000000000000	0.4987757068404410	T	T	T
0.2500000000000000	0.9964139459999970	0.2146293670000006	F	F	F
0.2500000000000000	0.9916158561626814	0.4987757068404410	T	T	T
0.2500000000000000	0.7500000000000000	0.2845222881816872	T	T	T
0.2500000000000000	0.7500000000000000	0.0008654109999995	F	F	F
0.9964139459999970	0.7500000000000000	0.0715431200000012	F	F	F
0.9934229461281825	0.7500000000000000	0.3578489359329504	T	T	T
0.2500000000000000	0.4964139759999995	0.0715431200000012	F	F	F
0.2500000000000000	0.4934229761281850	0.3578489359329504	T	T	T
0.2500000000000000	0.7500000000000000	0.1439516539999985	F	F	F
0.2500000000000000	0.7500000000000000	0.4303484423419060	T	T	T
0.0035860249999971	0.7500000000000000	0.2146293670000006	F	F	F
0.0083841148373126	0.7500000000000000	0.4987757068404410	T	T	T
0.2500000000000000	0.5035860540000030	0.2146293670000006	F	F	F
0.2500000000000000	0.5083841438373186	0.4987757068404410	T	T	T
0.7500000000000000	0.2500000000000000	0.2845222881816872	T	T	T
0.7500000000000000	0.2500000000000000	0.0008654109999995	F	F	F
0.4964139759999995	0.2500000000000000	0.0715431200000012	F	F	F
0.4934229761281850	0.2500000000000000	0.3578489359329504	T	T	T
0.7500000000000000	0.9964139459999970	0.0715431200000012	F	F	F
0.7500000000000000	0.9934229461281825	0.3578489359329504	T	T	T
0.7500000000000000	0.2500000000000000	0.1439516539999985	F	F	F
0.7500000000000000	0.2500000000000000	0.4303484423419060	T	T	T
0.5035860540000030	0.2500000000000000	0.2146293670000006	F	F	F
0.5083841438373186	0.2500000000000000	0.4987757068404410	T	T	T
0.7500000000000000	0.0035860249999971	0.2146293670000006	F	F	F
0.7500000000000000	0.0083841148373126	0.4987757068404410	T	T	T
0.7500000000000000	0.7500000000000000	0.0008654109999995	F	F	F
0.7500000000000000	0.7500000000000000	0.2888210346683538	T	T	T
0.5035860540000030	0.7500000000000000	0.0715431200000012	F	F	F
0.5065770538718175	0.7500000000000000	0.3578489359329504	T	T	T
0.7500000000000000	0.5035860540000030	0.0715431200000012	F	F	F
0.7500000000000000	0.5065770538718175	0.3578489359329504	T	T	T
0.7500000000000000	0.7500000000000000	0.1422208250000025	F	F	F
0.7500000000000000	0.7500000000000000	0.4280226560388691	T	T	T

0.4964139759999995 0.7500000000000000 0.2146293670000006 F F F
0.4916158861626839 0.7500000000000000 0.4987757068404410 T T T
0.7500000000000000 0.4964139759999995 0.2146293670000006 F F F
0.7500000000000000 0.4916158861626839 0.4987757068404410 T T T

M = Fe

1.00000000000000
8.0500000000000007 0.0000000000000000 0.0000000000000000
0.0000000000000000 8.0500000000000007 0.0000000000000000
0.0000000000000000 0.0000000000000000 28.1298873849000017
Sr Fe Ir O
16 8 8 48
Selective dynamics
Direct
0.0000000000000000 0.0000000000000000 0.0000000000000000 F F F
-0.0000000000000000 0.0000000000000000 0.2864278153983272 T T T
0.0000000000000000 0.0000000000000000 0.1430862400000024 F F F
-0.0000000000000000 0.0000000000000000 0.4321129091169274 T T T
0.0000000000000000 0.5000000000000000 0.0000000000000000 F F F
-0.0000000000000000 0.5000000000000000 0.2864278153983272 T T T
0.0000000000000000 0.5000000000000000 0.1430862400000024 F F F
-0.0000000000000000 0.5000000000000000 0.4321129091169274 T T T
0.5000000000000000 0.0000000000000000 0.0000000000000000 F F F
0.5000000000000000 0.0000000000000000 0.2864278153983272 T T T
0.5000000000000000 0.0000000000000000 0.1430862400000024 F F F
0.5000000000000000 0.0000000000000000 0.4321129091169274 T T T
0.5000000000000000 0.5000000000000000 0.0000000000000000 F F F
0.5000000000000000 0.5000000000000000 0.2864278153983272 T T T
0.5000000000000000 0.5000000000000000 0.1430862400000024 F F F
0.5000000000000000 0.5000000000000000 0.4321129091169274 T T T
0.2500000000000000 0.2500000000000000 0.2146293670000006 F F F
0.2500000000000000 0.2500000000000000 0.4973626071614730 T T T
0.2500000000000000 0.7500000000000000 0.0715431200000012 F F F
0.2500000000000000 0.7500000000000000 0.3555461238288824 T T T
0.7500000000000000 0.2500000000000000 0.0715431200000012 F F F
0.7500000000000000 0.2500000000000000 0.3555461238288824 T T T
0.7500000000000000 0.7500000000000000 0.2146293670000006 F F F
0.7500000000000000 0.7500000000000000 0.4973626071614730 T T T
0.2500000000000000 0.2500000000000000 0.0715431200000012 F F F
0.2500000000000000 0.2500000000000000 0.3573147725189098 T T T
0.2500000000000000 0.7500000000000000 0.2146293670000006 F F F
0.2500000000000000 0.7500000000000000 0.4977936103762828 T T T
0.7500000000000000 0.2500000000000000 0.2146293670000006 F F F
0.7500000000000000 0.2500000000000000 0.4977936103762828 T T T
0.7500000000000000 0.7500000000000000 0.0715431200000012 F F F
0.7500000000000000 0.7500000000000000 0.3573147725189098 T T T
0.2500000000000000 0.2500000000000000 0.0008654109999995 F F F
0.2500000000000000 0.2500000000000000 0.2866211769926554 T T T
0.0035860249999971 0.2500000000000000 0.0715431200000012 F F F
0.0018862664198085 0.2500000000000000 0.3574738235618511 T T T
0.2500000000000000 0.0035860249999971 0.0715431200000012 F F F
0.2500000000000000 0.0018862664198085 0.3574738235618511 T T T
0.2500000000000000 0.2500000000000000 0.1422208250000025 F F F
0.2500000000000000 0.2500000000000000 0.4278141863719814 T T T
0.9964139459999970 0.2500000000000000 0.2146293670000006 F F F
0.9950264937798349 0.2500000000000000 0.4998392206916381 T T T
0.2500000000000000 0.9964139459999970 0.2146293670000006 F F F
0.2500000000000000 0.9950264937798349 0.4998392206916381 T T T
0.2500000000000000 0.7500000000000000 0.2854873482051603 T T T
0.2500000000000000 0.7500000000000000 0.0008654109999995 F F F
0.9964139459999970 0.7500000000000000 0.0715431200000012 F F F
0.9981137045801856 0.7500000000000000 0.3574738235618511 T T T
0.2500000000000000 0.4964139759999995 0.0715431200000012 F F F
0.2500000000000000 0.4981137345801880 0.3574738235618511 T T T
0.2500000000000000 0.7500000000000000 0.1439516539999985 F F F
0.2500000000000000 0.7500000000000000 0.4288020486807506 T T T
0.0035860249999971 0.7500000000000000 0.2146293670000006 F F F

0.0049734772201590	0.7500000000000000	0.4998392206916381	T	T	T
0.2500000000000000	0.5035860540000030	0.2146293670000006	F	F	F
0.2500000000000000	0.5049735062201651	0.4998392206916381	T	T	T
0.7500000000000000	0.2500000000000000	0.2854873482051603	T	T	T
0.7500000000000000	0.2500000000000000	0.0008654109999995	F	F	F
0.4964139759999995	0.2500000000000000	0.0715431200000012	F	F	F
0.4981137345801880	0.2500000000000000	0.3574738235618511	T	T	T
0.7500000000000000	0.9964139459999970	0.0715431200000012	F	F	F
0.7500000000000000	0.9981137045801856	0.3574738235618511	T	T	T
0.7500000000000000	0.2500000000000000	0.1439516539999985	F	F	F
0.7500000000000000	0.2500000000000000	0.4288020486807506	T	T	T
0.5035860540000030	0.2500000000000000	0.2146293670000006	F	F	F
0.5049735062201651	0.2500000000000000	0.4998392206916381	T	T	T
0.7500000000000000	0.0035860249999971	0.2146293670000006	F	F	F
0.7500000000000000	0.0049734772201590	0.4998392206916381	T	T	T
0.7500000000000000	0.7500000000000000	0.0008654109999995	F	F	F
0.7500000000000000	0.7500000000000000	0.2866211769926554	T	T	T
0.5035860540000030	0.7500000000000000	0.0715431200000012	F	F	F
0.5018862954198144	0.7500000000000000	0.3574738235618511	T	T	T
0.7500000000000000	0.5035860540000030	0.0715431200000012	F	F	F
0.7500000000000000	0.5018862954198144	0.3574738235618511	T	T	T
0.7500000000000000	0.7500000000000000	0.1422208250000025	F	F	F
0.7500000000000000	0.7500000000000000	0.4278141863719814	T	T	T
0.4964139759999995	0.7500000000000000	0.2146293670000006	F	F	F
0.4950265237798375	0.7500000000000000	0.4998392206916381	T	T	T
0.7500000000000000	0.4964139759999995	0.2146293670000006	F	F	F
0.7500000000000000	0.4950265237798375	0.4998392206916381	T	T	T

References

1 D. J. Chadi, *Phys. Rev. B*, 1977, **16**, 1746–1747.

2 I. C. Man, H. Y. Su, F. Calle-Vallejo, H. A. Hansen, J. I. Martínez, N. G. Inoglu, J. Kitchin, T. F. Jaramillo, J. K. Nørskov and J. Rossmeisl, *ChemCatChem*, 2011, **3**, 1159–1165.

3 A. Govind Rajan, J. M. P. Martirez and E. A. Carter, *ACS Catal.*, 2020, **10**, 11177–11234.

4 L. C. Seitz, C. F. Dickens, K. Nishio, Y. Hikita, J. Montoya, A. Doyle, C. Kirk, A. Vojvodic, H. Y. Hwang, J. K. Norskov and T. F. Jaramillo, *Science*, 2016, **353**, 1011–1014.

5 J. Varignon, M. Bibes and A. Zunger, *Nat. Commun.*, 2019, **10**, 1–11.

6 W. Tang, E. Sanville and G. Henkelman, *J. Phys. Condens. Matter*, 2009, **21**, 084204.

7 A. Walsh, A. A. Sokol, J. Buckeridge, D. O. Scanlon and C. R. A. Catlow, *Nat. Mater.*, 2018, **17**, 958–964.

8 A. Walsh, A. A. Sokol, J. Buckeridge, D. O. Scanlon and C. R. A. Catlow, *J. Phys. Chem. Lett.*, 2017, **8**, 2074–2075.

9 R. D. Shannon, *Acta Crystallogr. Sect. A*, 1976, **32**, 751–767.

10 P. Kayser, J. A. Alonso, F. J. Mompeán, M. Retuerto, M. Croft, A. Ignatov and

M. T. Fernández-Díaz, *Eur. J. Inorg. Chem.*, 2015, **2015**, 5027–5038.

11 P. Kayser, M. J. Martínez-Lope, J. A. Alonso, M. Retuerto, M. Croft, A. Ignatov and M. T. Fernández-Díaz, *Inorg. Chem.*, 2013, **52**, 11013–11022.

12 C. C. L. McCrory, S. Jung, J. C. Peters and T. F. Jaramillo, *J. Am. Chem. Soc.*, 2013, **135**, 16977–16987.

13 S. Trasatti and O. A. Petrii, *J. Electroanal. Chem.*, 1992, **327**, 353–376.